In vivo Optical Projection Tomography (OPT) in *Caenorhabditis elegans*

Matthias Rieckher*

Supervisors: Dr. Nektarios Tavernarakis* and Dr. Jorge Ripoll[+]

Co-elaborator: Heiko Meyer[+]

*Institute of Molecular Biology and Biotechnology (IMBB),
Foundation of Research and Technology Hellas (FORTH)

[+]Institute of Electronic Structure and Laser (IESL),
Foundation of Research and Technology Hellas (FORTH)

Table of contents

Summary

Small sample spatial *in vivo* imaging techniques such as confocal microscopy, micro MRT (μMRT), Selective Plane Illumination Microscopy (SPIM) or contrast enhanced techniques such as DICM (Differential Interference Contrast Microscopy) are common tools for imaging fluorescent expression in the nematode *Caenorhabditis elegans*. However, these methods have limited capacity for high resolution, rapid, whole body 3D microscopic imaging and/or imaging of multiple contrast agents.

The recently developed approach of Optical Projection Tomography (OPT) enables 3D visualization of whole specimens up to several millimetres in size as has already been shown in zebra fish, chick and mouse embryos. This is achieved by applying a filtered back projection algorithm on images taken from equidistant angles of a rotating specimen with magnification dependent resolution, down to 1-5 μm. Here I present a modified OPT setup for 3D imaging of GFP expressing neuronal cells in *C. elegans*. This study demonstrates that this novel technique allows rapid acquisition of whole-animal fluorescent expression patterns in the nematode with high accuracy. OPT visualization can easily be adapted to image multiple tissues and cell types, with a variety of chromophores, that allow multi-colour projections, in the nematode.

Introduction

The model organism *Caenorhabditis elegans*

Caenorhabditis elegans (*C. elegans*) is an ideal simple model organism for genetic and molecular studies and additionally has proved to be a highly relevant model for studying human disorders, such as neurodegenerative diseases (Driscoll and Gerstbrein 2003).

C. elegans shows a very simple anatomy: the total number of cells of the animal is 959, including 302 neurons that form a simple nervous system. The cell lineage in development of the nematode is fully deciphered and a complete lineage tree is available (see http://www.wormatlas.org/; Sulston et al. 1983). During development, 131 cells which undergo programmed cell death (Ellis and Horvitz 1986). This makes *C. elegans* a powerful tool for investigating developmental biology (Bargmann and Avery 1995).

An important advantage of the nematode is its transparency, which makes microscopy far easier, permitting every cell division throughout development to be tracked. The simple nervous system is well documented, all neurons are mapped and an almost complete wiring diagram has been created (see http://www.wormatlas.org/; White et al. 1983; Hall and Russell 1991). Specific behaviors, such as locomotion, chemo- or thermotaxis, as well as learning and memory, can be experimentally associated with the relevant neuron(s) (Thomas and Lockery 2005). The detailed characterization of its nervous system renders *C. elegans* particularly suited for the study of neurodegeneration and ageing (Murakami 2007).

C. elegans develops from the fertilized egg to a self-fertilizing adult hermaphrodite within 3.5 days by undergoing four larval stages (L1 to L4). Due to food starvation or harsh environmental conditions the developing larva can enter a so-called, dauer stage before completing the L1 stage, which increases the mean life span for more than 5 months. Favourable food conditions allow the animal to re-enter the normal life cycle as an L4 larva. After entering the adult stage an approximately three day reproductive period follows, during which the animal lays about 300 eggs. *C. elegans* lives around 20 days, of which the last two weeks are characterized by a decline in locomotion, food pumping and recognizable tissue degeneration, revealing typical symptoms of ageing. A low percentage of male animals (about 0.1 % of the progeny) are generated by hermaphrodites during self fertilization. These males

enable genetic crosses that allow easy construction of double or multiple mutants (Riddle et al. 1997). Due to its short life span, the nematode is particularly popular for studying the mechanisms of ageing and senescent decline (Lim et al. 2006).

Another important advantage of the animal is the easy maintenance in the laboratory. *C. elegans* feeds on bacteria (usually *Escherichia coli* strain OP50), which are grown either on solid agar plates or in liquid culture medium, and grows best at a temperature of 20°C (Brenner 1974). The culturing temperature affects development timing: For example, *C. elegans* grows about 30% slower at 16°C compared to 20°C, making it convenient to time experimental procedures. The nematode can be cultured on large scale.

The *C. elegans* genome has been fully sequenced and annotated and a physical map of the genome based on the use of cosmids and yeast artificial chromosomes (YACs) has been created (Waterston and Sulston 1995). The *C. elegans* genome is organized in 5 autosomes plus the sex chromosome X (sequence database: http://www.wormbase.org/) and approximately 20.000 open reading frames (ORFs) for the nematode have been predicted (Blumenthal et al. 2002). Additionally detailed protein interaction networks have been modelled (Walhout et al. 2000).

The availability of fully charted genomes allows the implementation of large-scale, genome-wide genetic and molecular methodologies such as double stranded RNA mediated interference (dsRNAi; (Mello and Conte 2004). In *C. elegans*, high-throughput RNAi screens against all 20.000 ORFs have been published (Simmer et al. 2003). The use of dsRNAi in the nervous system of the nematode has been less successful so far, but can be offset by the use of special hypersensitive mutants or the introduction of double-stranded hairpin RNAs (dshRNAs) through microinjection (Tavernarakis et al. 2000; Schmitz et al. 2007).

C. elegans is genetically malleable (Lee et al. 2004). The most straightforward method of creating mutants is random mutagenesis through the use of the chemical ethyl methanesulfonate (EMS). Mutants for almost every gene are available and can be ordered from stock centers. Animals carrying multiple mutations can be constructed and efficient genetic mapping is possible, by utilizing precise single nucleotide polymorphism (SNP) maps available for the model organism (Jakubowski and Kornfeld 1999).

Transgenic animals can be obtained by microinjection of engineered DNA samples into the gonad, where they generate inherited extrachromosomal arrays.

This extrachromosomal array can further be integrated and stabilized in the genome through mutagenesis-induced integration (Mello and Fire 1995; Jin 2005).

In summary, *C. elegans* is a widely used model organism to study all kinds of biological phenomena, like development, ageing, learning and memory, and it serves as a platform to investigate the molecular mechanisms of human diseases, such as pathogenic, muscle disorder or neurodegenerative diseases.

C. elegans in 3D microscopy

A fundamental advantage of *C. elegans* as a model organism is its transparency which allows deep point focussing through standard 2 dimensional (2D) microscopy techniques such as low-magnification stereomicroscopy, and high-magnification compound and confocal microscopy (Schnabel 2005).

However, there is need for 3 dimensional (3D) whole animal imaging in the nematode which allows digital sectioning of a sample. This would be a useful tool to reveal the anatomical structure and to visualize fluorescent gene expression patterns of transgenic animals. Optical sectioning techniques on *C. elegans* have been performed on the basis of serial-section reconstruction, laser scanning confocal microscopy (LSCM) and micro Magnetic Resonance Imaging (μMRI). Nevertheless, these techniques show limitations of applications in the nematode:

LSCM has the ability to produce in-focus 3D images of small specimens which is called optical sectioning. Images are acquired point-by-point and reconstructed by certain computer programs, which also allows three-dimensional reconstructions of the sample. In LSCM, a laser beam passes through a light source aperture and objective lens focuses the light into a small area within the fluorescent specimen. The principle of the technique is that out-of-focus light is suppressed by passing through a pinhole, resulting in a sharp focused image. The use of a beam splitter allows only the laser light to pass to the photodetection device. Obtaining and digitally assembling images of various z axis planes (z stacks) through a specimen further permits the reconstruction of a 3D picture (Paddock 1999). So, confocal microscopy allows visualization and 3D reconstructions on subcellular level but is limited when it comes to whole-animal recording. In *C. elegans*, confocal miscroscopy has for example been used to visualize GFP and yellow fluorescent protein (YFP) labelled microtubule to study the process of cell division (Kozlowski et al. 2007).

Another commonly used technique mainly for developmental studies in the nematode is 4D embryo imaging through a multifocal plane time-lapse video recording system (Hird and White 1993). Multiple layers of the embryo are recorded through Differential Interference Contrast Microscopy (DICM, also called Nomarsky microscopy) in certain time intervals. The received information about positioning of single cells is manually represented in 4D which is supported by standard used software such as SIMI Biocell^{TM} (Schnabel et al. 1997). This allows improved cell lineage representations and precise studies of embryonic strategies such as pattern formation through cell sorting (Bischoff and Schnabel 2006; Schnabel et al. 2006). These techniques have been further improved by fluorescently labelled nuclei which can be tracked more easily (Bao et al. 2006). Through the use of fluorescent labels the expression of certain genes can be followed up to the 350 cell stage of development and high-throughput methods have been applied (Bao et al. 2006; Hunt-Newbury et al. 2007). Nevertheless, this technique neither produces real 3D images nor allows *in silico* sectioning of the nematode.

The technique μMRI offers the possibility to view whole specimen and even gene expression patterns *in vivo*. A strong magnetic field is used to align the nuclear magnetization of hydrogen atoms of the sample resulting in a 3D image. Nevertheless, resolution and recording of fluorescence of the technique are strongly limited (Pautler and Fraser 2003). The method proves to be inefficient to visualize *C. elegans* in satisfying resolution.

Another technique that makes *in vivo* optically sectioning throughout specimen of several mm in size possible is SPIM: The technique offers optical sectioning, reduced fluorophore bleaching, fast, highly efficient image recording, and high depth penetration, especially when multiple views are combined. SPIM performs well in large samples such as fish or fly embryos, which can be observed *in vivo* for several days. The method is based on optical sectioning by laser scanning microscopy in this case achieved through illuminating the sample along a separate optical path orthogonal to the detection axis (Huisken et al. 2004). The SPIM principles are universal and have been successfully applied using objective lenses with high magnification, covering sample sizes from 20 μm to 1 mm with isotropic resolutions from 5μm to 300 nm. So far no application in *C. elegans* has been published although the method is used e.g. to observe gene expression patterns in the nematode (Sarov personal communication).

Recently, a new method called optical projection tomography (OPT) has proven capability to produce rapid high resolution 3D visualization of small specimen of 1 to 10 mm in size (Sharpe et al. 2002). This technique fills the gap between μMRI and confocal microscopy. OPT uses projections from different angles perpendicular to the rotational axis of the specimen undergoing one full revolution. The use of standard convolution filtered back projection of each projection yields a reconstruction of all slices. Thereby 3D volumetric representation of the specimen of either the fluorescence patterns or anatomical information or a combination of multiple channels is received (Sharpe 2003). For a closer explanation of the technique see figures 1 and 2. This technique has already been successfully shown to produce high quality 3D imaging of fixed chick and mouse embryos (Sharpe et al. 2002; Arques et al. 2007), plants (Lee et al. 2006), zebra fish (Bryson-Richardson et al. 2007), *Drosophila melanogaster* (McGurk et al. 2007) and the developing human brain (Sarma et al. 2005).

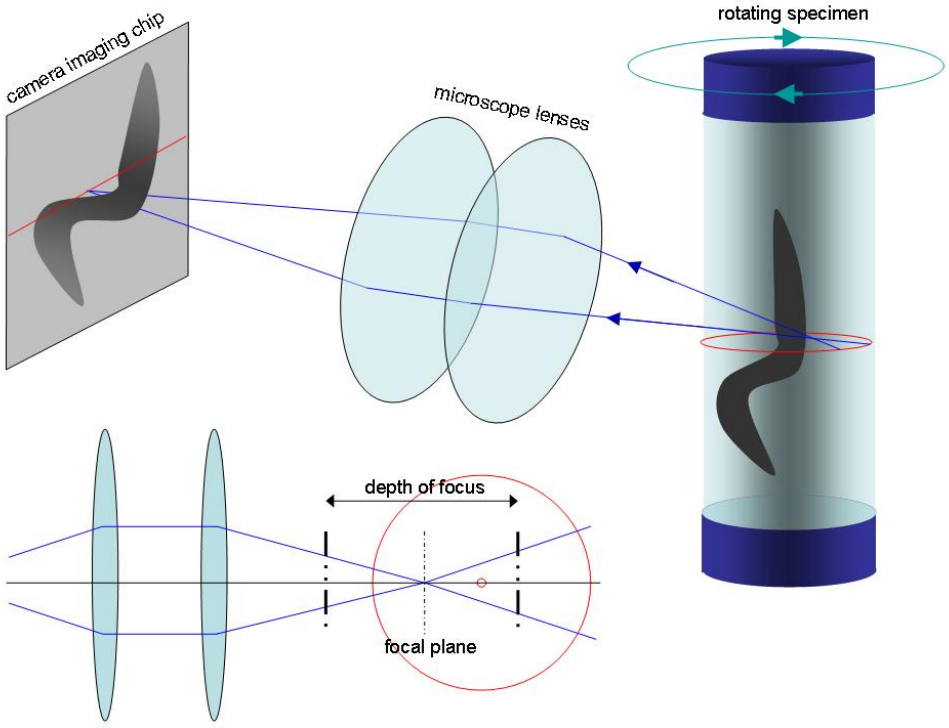

Figure 1: OPT microscopy in general. The upper image shows a schematic of the OPT microscopy setup. The specimen is fixed and rotated within a cylinder of agarose for imaging by a microscope. A camera imaging chip (CIC) collects the transmitted light from the specimen. The whole apparatus is adjusted so that light emitted from a slice perpendicular to the rotation axis is focused onto a single row of pixels on the CIC. This slice is indicated by a red ellipse and a red line. In the picture down the red circle represents this slice and shows the principle of OPT out of-focus imaging: Basically, in contrast to confocal microscopy in which out-of-focus light is suppressed, in OPT these regions outside the focal plane are collected. By turning and recording images of the specimen in equidistant angles through full 360 degrees many focus and out-of focus data are collected and later combined (modified from Sharpe et al. 2002).

small of
depe on
ns

and a protocol for sample preparation is applied. To prove this, we analyze the fluorescent expression patterns [green fluorescent protein (GFP), dsRED and merged images] of several genes expressed in specific neurons of the nematode. The technique allows rapid 3D visualization in high resolution and proves to be a powerful tool to define anatomical features and gene expression patterns of *C. elegans*.

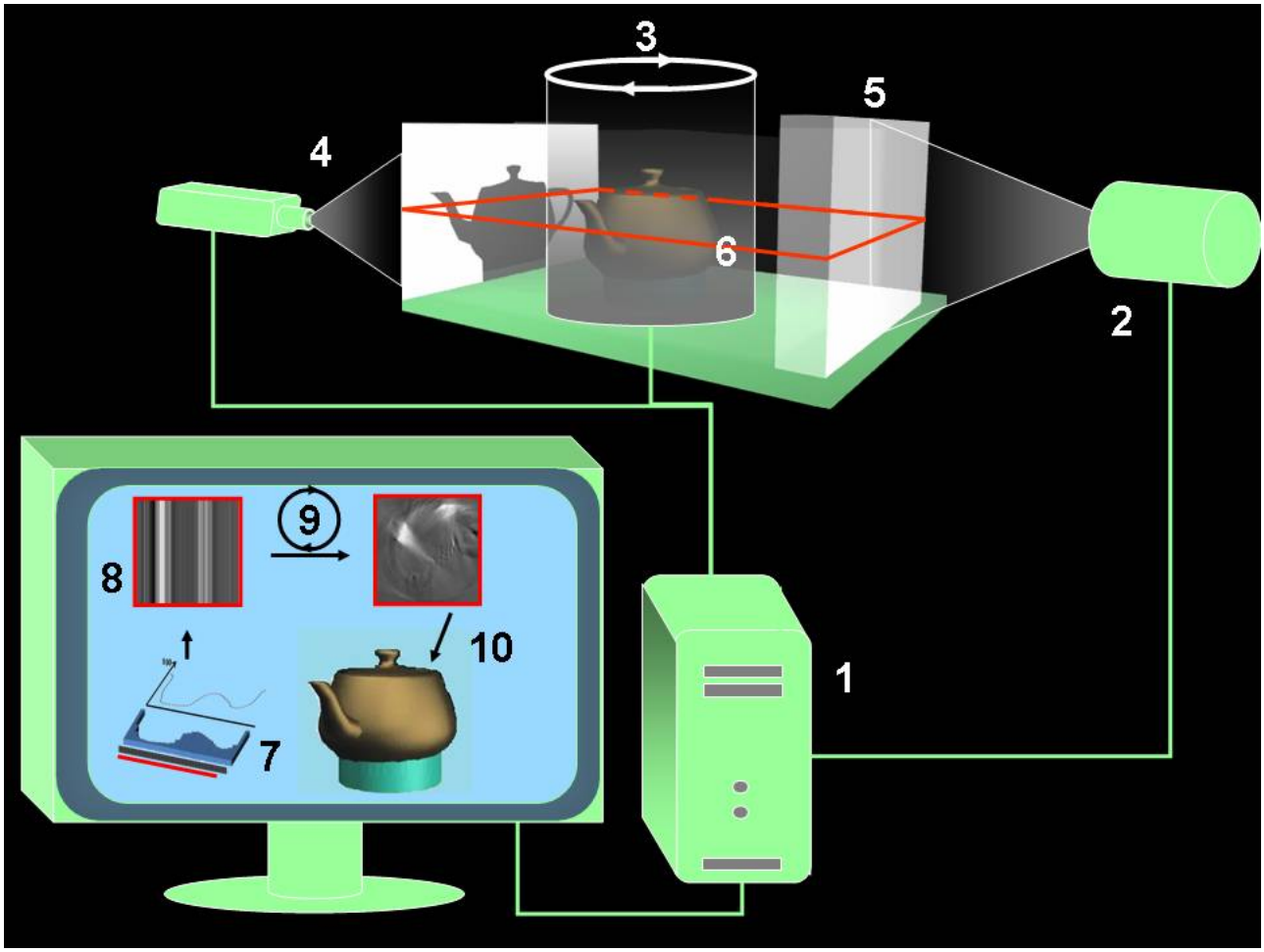

Figure 2: Principles of the OPT method in practice. A PC (1) is controlling the light source (laser; 2), the stepper motor (3), turning the sample and the ICCD camera (4). The light is diffused by a diffuser (5) and shines through the object. In principle, the shadow of the object is collected by the camera in slices of pixel lines (6). These data are then changed into a line integral (7) by a custom made program based on LabView™ through a standard convolution backprojection algorithm and result in raw data images. After rotating the object and capturing raw data from several equidistant angles (8), the pictures are merged into a denser image (9). Through the use of freeware such as MRIcro or MRIcroN the final 3D image can be obtained and processed (10).

Materials and Methods

Sample preparation for *in vivo* measurements

C. elegans maintenance and creation of transgenic animals was done as described previously (Brenner 1974). In our studies we used the following constructs for 3D imaging: Ex[$_{daf\text{-}6}$GFP $_{pqn\text{-}21}$dsRed pRF4] and Ex[$_{unc\text{-}8}$GFP pRF4].

Capillaries were either used in original shape or modified using a capillary puller (PN-30, Narishige Co.LTD., *Tokyo, Japan*). The tip was tapered to reduce the inner diameter for enhanced stability of sample positioning.

Young adult worms were anaesthetized by incubation for 15 min in 20 mM sodium azide (NaN_3, Merck, *Darmstadt, Germany*) solution at 20°C or room temperature and then transferred in a drop of halocarbon oil (Sigma-Aldrich Co., *St. Louis, MO, USA*). Rests of anaesthetic were removed by moving the worm in the oil with a hairpin. Animals were the soaked into the tip of the capillary by a mouth pipette. The capillary was carefully cleaned with 70% ethanol and then sealed by slightly dipping into liquid glue (Glue-All, Multi-Purpose Glue, Elmer's Products Inc., *Columbus, OH, USA*) and air dried at room temperature for 5 min.

Experimental Setup

The system (see figure 3) consists of two DPSS Lasers (100mW cw, 473nm and 30mW cw, 532nm, Laserlight, *Berlin, Germany*), an ultra fast laser shutter (LS 6, UniBlitz, *Rochester, NY, USA*), and optional a 5x beam expander (Edmund Optics Inc., *Karlsruhe, Germany*) to enlarge the beam from 2mm to 10mm spot size for quasi homogeneous illumination of the area of interest. The sample holder is based on a high resolution rotation system, containing a high resolution stepper motor (Oriental Motors) with 500 steps per revolution with a custom made capillary holder holding standard single use micro capillaries (Blaubrand® - intraMARK, BRAND GmbH, *Wertheim, Germany*) immersed in a custom made index matching vessel using 50x24x0.15 mm borosilicate cover slips (n_w = 1.474) containing 87% glycerol solution (FLUKA) (Sigma-Aldrich Co., *St. Louis, MO, USA*) as an index matching fluid (n_f = 1.474) to minimize internal reflections and refraction of the excitation and emission light. The imaging unit consists of a lens tube system (InfiniTube™, Infinity, *Boulder, CO, USA*) containing a custom made filter slide containing 25 mm dia.

fluorescence filters (525 ± 17.5nm for GFP, 593 ± 20nm for DsRed, both Semrock, *Rochester, NY, USA*) and optional a 5x or alternatively a 10x infinity corrected microscope objective (Mitutoyo, *Kawasaki, Japan*) and a TE cooled intensified CCD with 1002 x 1004 pixel (ANDOR Technology, *Belfast, Northern Ireland*). To increase the focal depth of the system, a variable aperture (iris) has been placed behind the objective according to Ripoll et al "in focus measurements with small apertures" (Ripoll and Ntziachristos 2004).

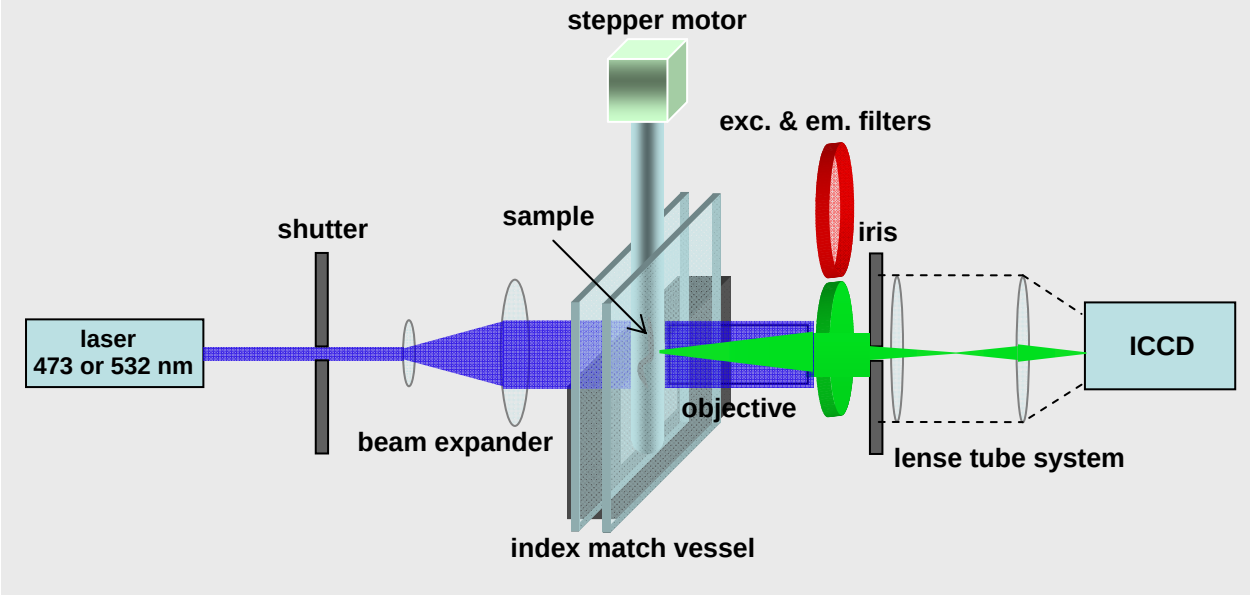

Figure 3: Schematic drawing of the OPT setup containing laser, shutter, beam expander, stepper motor, capillary mount with micro capillary and sample, index matching vessel, microscope objective, filter slide with fluorescence filters, variable aperture (iris), lens tube system and an ICCD camera. The light beam is indicated in blue and green.

Data acquisition

Raw data acquisition took place under use of the custom programmed software called "Main_Control", based on LabView™ controlling the camera, the stepper motor, the laser shutter with a 3.6 GHz PC with 2GB RAM required for the fast data acquisition feature of the camera. The needle including the sample was placed into a holder connected to the stepper motor and a certain plane within the specimen is focused. By turning the sample in 45° steps this focal plane was then adjusted for a whole revolution. After assigning the equidistant angle steps (0.72°), the final number of angels (500), the excitation times (0.07 to 0.1 sec for white light

and between 1.0 and 5.0 sec for fluorescent signals) and the certain emission filters (GFP or dsRed), the recording was started and executed automatically. A first record was performed to capture fluorescent images (two records for two different fluorescent dyes, respectively) and a second for the white light image.

3D reconstructions were done through the custom-made program, “Process Main – Radon transform”, which is based on LabView™. Further processing of the reconstructed data and merges were accomplished through “ImageJ – Image Processing and Analysis in Java, version 1.38x” and the 3D visualization happened either through “MRIcro, version 1.40” or “MRIcroN”.

Results

Recording raw data

Worms were prepared and recorded as described in Materials and Methods. The first step was the record of 500 2D white light images of the rotating *C. elegans* hermaphrodite sample from equidistant angles in 0.72° steps. The specimen is embedded in halocarbon oil in a pulled capillary. In first experiments we used a 2% low melting agarose and 10 mM NaN_3 to embed *C. elegans* as previously done in OPT based 3D imaging of *Drosophila*. In those protocols whole animal samples were mounted in 1% agarose, dehydrated in methanol and then cleared in BABB (1 part Benzyl Alcohol: 2 parts Benzyl Benzoate) (McGurk et al. 2007). Fortunately, the clearing step is not necessary in *C. elegans* due to the transparency of the animal. This makes in vivo 3D imaging possible. The use of halocarbon oil proves to be more efficient since its refractory index is close to the one of the capillary glass which results in pictures of higher resolution.

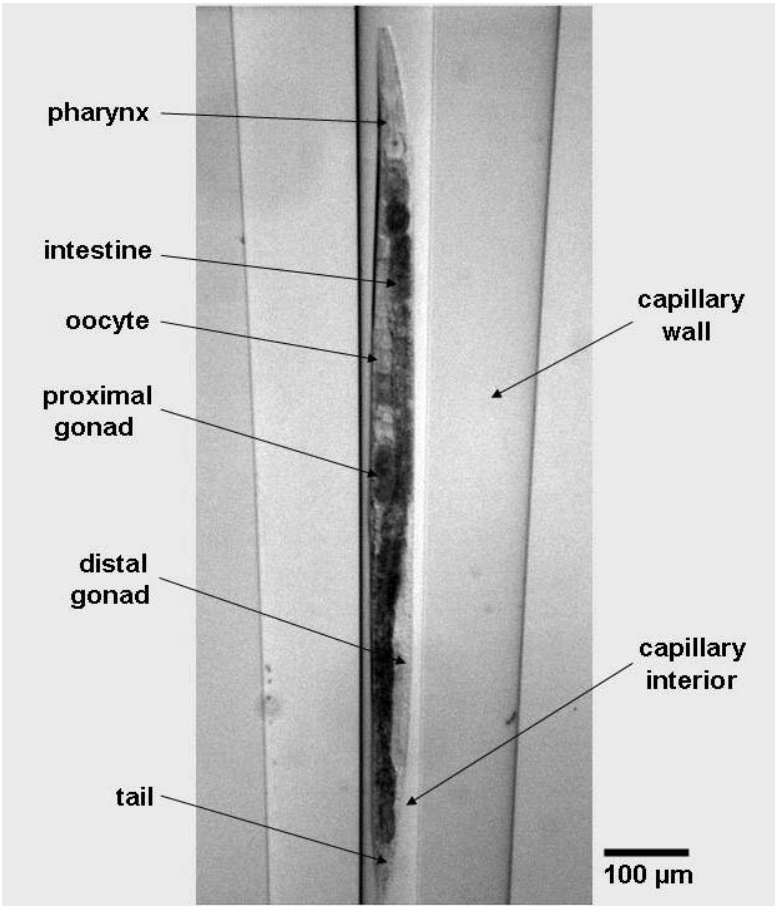

Figure 4: OPT raw data image of C. elegans *in the capillary. The picture shows the first of 500 white light images taken through a 5x lens. The focal plane is localized in the centre of the worm and anatomical features are visible and indicated by arrows. A file containing 500 of these images recorded from equidistant angles (0.72° each) is considered as raw data and will be further processed for reconstruction.*

The white light images mainly serve as standard background image to merge with fluorescent signals. Nevertheless, anatomical features can be observed and with a 5x microscope lens tissues and organs can be distinguished (see figure 4). One record of white light images resulted in approximately 1 GB of data size. Since the excitation time usually was much less then 0.1 sec one full rotation took less then 5 min. Raw data were then further reconstructed into 3D data. The final resolution was about 1-5 µm.

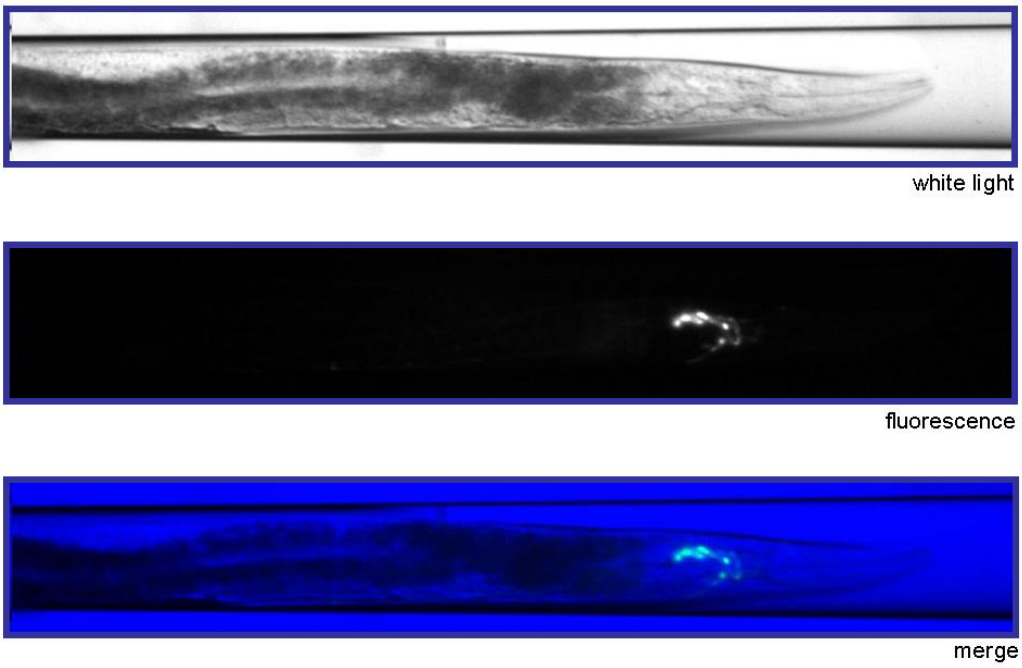

Figure 5: OPT raw data images. 500 pictures each from equidistant angles were taken through a 10x lens for white light and GFP fluorescence images and merged through the program ImageJ. White light and fluorescence raw data were processed further for 3D reconstruction. The figure shows the expression of GFP under the control of the unc-8 *promoter with a strong signal in the pharynx region.*

To record fluorescent 3D images another rotation of the sample was performed by exciting the fluorescent dyes GFP and dsRed by a laser beam combined with the according emission filters, respectively. Besides, exactly the same settings as in the white light image record were applied. One full rotation depending on the proper excitation time took between 500 sec and 2500 sec. The longer the excitation time, the higher the possibility of sample movement due to different factors (see Discussion). In principle, recording of fluorescent and white light images delivering the necessary raw data including the time of preparing, focussing and recording the sample took less then 30 min.

Sample and capillary had to be fixed stable in position in order to achieve a correct merged image (see figure 5). Anaesthetizing the nematode prior to the record through incubation in NaN_3 caused complete immobility. Records were observed for possible movements of both capillary and specimen through visualizing the picture stack in ImageJ. Movement during the recording could not be compensated through the used software for the 3D reconstructions and experiments had to be redone. For testing the setup sample specimen were reused for several test runs. The size of the received data was about 1 GB as in the white light image stack. Recorded raw data were then reconstructed into 3D data.

Acquisition of 3D images

Recorded raw data were further processed into 3D data through the use of a custom made program based on LabView™. The program Radon::Main Radon transform allows the visualization of the raw data images and the choice of a specific region for reconstruction into 16 bit image data. First the program automatically calculated the centre of rotation which then had to be manually adjusted. After initiation of the process, the raw data of the sample were reconstructed slice by slice and assembled. Depending on the size of the area to be reconstructed the procedure took between some min and several hours for whole samples. Further the choice of different reconstruction filters possibly improved the quality of the reconstructed data.
The received image data then were further progressed through 3D visualization programs such as MRIcro or MRIcroN. Those programs mainly allow *in silico* sectioning of the specimen along the coronal, transversal and sagittal plane in up to 1002 slices. Also, the picture can be cropped and adjusted and unwanted parts such as the capillary wall can be digitally removed (see figures 6 to 8). Rendering features can be applied in order to visualize the specimen in 3D space and remove layers (data not shown).

White light 3D images

White light images were reconstructed as template for merge with the fluorescent reconstruction. After reconstruction and visualization of pictures taken through a 10x microscopy lens all anatomical features of *C. elegans* were visible in high resolution and quality images (see figure 6). *In silico* sectioning was performed to demonstrate the power of the 3D imaging technique: Oocytes, intestine, cuticle and the subregions of the pharynx can easily be recognized. The resolution is about 5 to 10 µm.

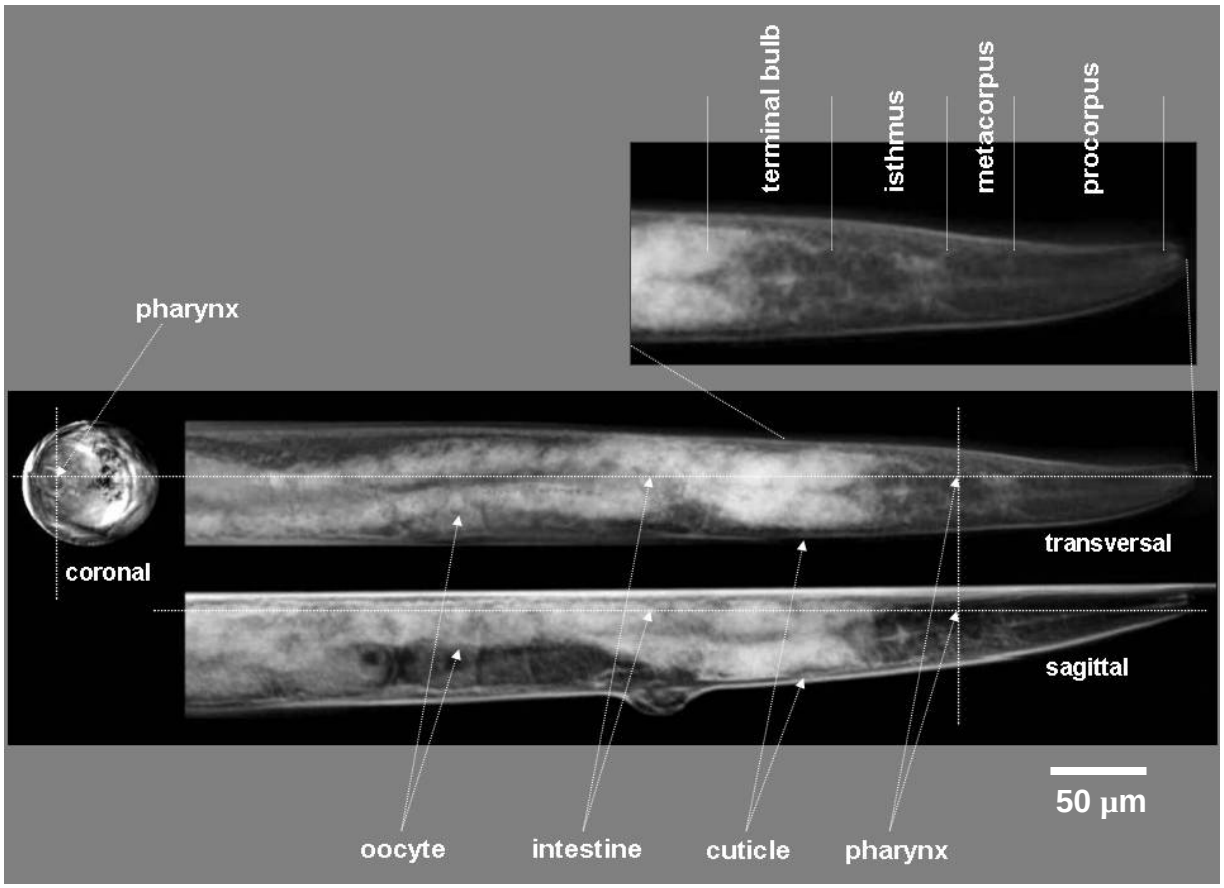

Figure 6: In silico *slice through* C. elegans*. After processing the raw data into 3D reconstructions, those data can be viewed by software such as MRIcro or MRIcroN. The 3D picture based on white light images of the anterior part of the nematode (recorded through 10x lens) can be sectioned* in silico *and reveals anatomical features (indicated by arrows). In this case slice 928 is shown in the coronal, transversal and sagittal view (see white line). The pharynx is digitally magnified.*

Expression of GFP

A major goal in applications for OPT microscopy is the 3D visualization of fluorescent expression patterns. Reconstructed white light and fluorescent image data were merged and *in silico* sectioning was performed to reveal the localization of expression. To demonstrate the functionality of the technique in these terms, worms stably expressing GFP under the control of the *unc-8* promoter were reconstructed and the expression pattern was compared to previously published data. The *unc-8* gene is expressed in neurons localized in the nerve ring at the pharynx and in motorneurons along the body (Tavernarakis et al. 1997). Figure 7 shows slice 928 in coronal, sagittal and transversal plane. The OPT method seems to be sufficient to show the expression of GFP by the *unc-8* promoter in the expected pattern: Signals were observed in the pharynx region (see figure 7) and in other *in silico* slices in the motorneurons (data not shown).

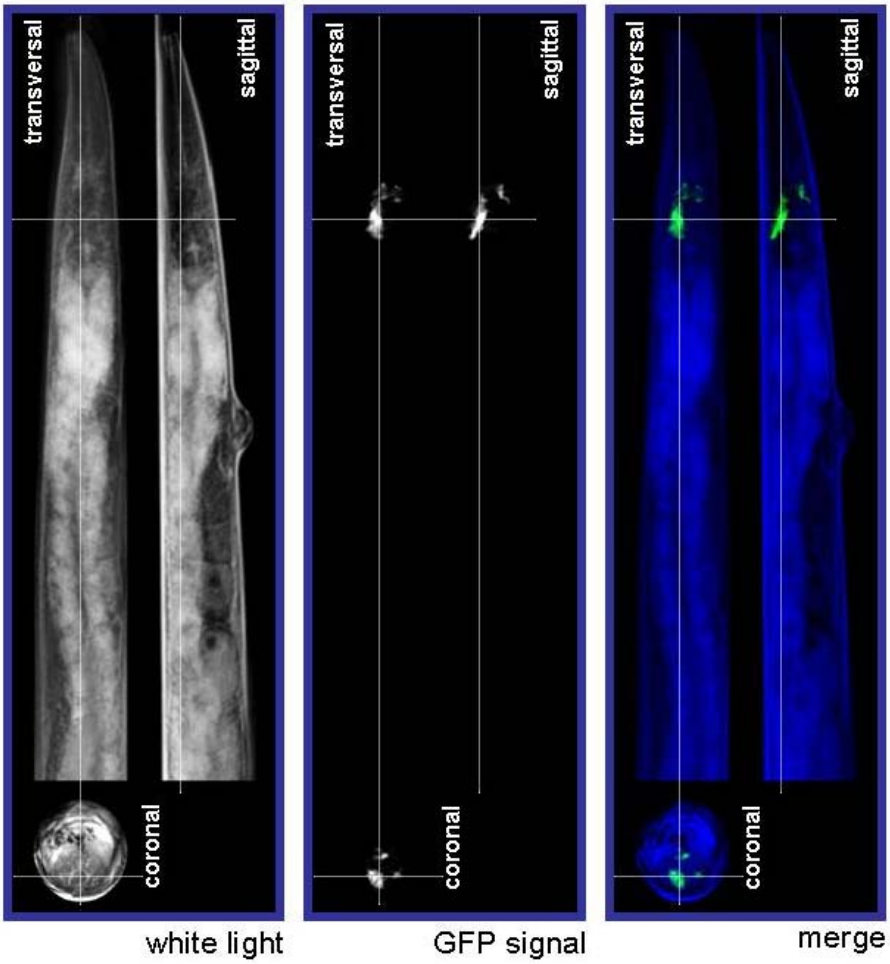

Figure 7: In silico *slice through* C. elegans*. White light image as in figure 6, GFP signal and merge of 3D reconstructed data. GFP is expressed under the control of the* unc-8 *promoter. Slice 928 is shown in the coronal, transversal and sagittal view (see white line).*

Co-expression of GFP and dsRed

To show the ability of OPT to measure signals from two different fluorescent dyes, animals were recorded the stably co-express GFP and dsRed under the control of different promoters: the GFP labelled *daf-6* promoter is expressed in the amphid sheath glia, the phasmid sensory organ sheath and socket cells, cells of the excretory system and the vulva (Perens and Shaham 2005). The fluorescent protein dsRed was put under the control of the *pqn-21* promoter which expresses in almost all somatic cells. The expression of those genes has been found to co-localize in some cells in the pharynx region (Bazopolou personal communication). The co-localization was proven through use of the OPT method in at least one case by visualizing slice 945 (see figure 8). The picture taken by fluorescent light microscopy

(see figure 9) shows co-localization of the patterns in some cells (yellow) of the pharynx region and mainly the expected co-expression in the excretory canal cell (highlighted region, figure 9). This co-localization can also be seen in the OPT 3D images and the merged cell can possibly identified as the excretory canal cell (highlighted region, figure 8).

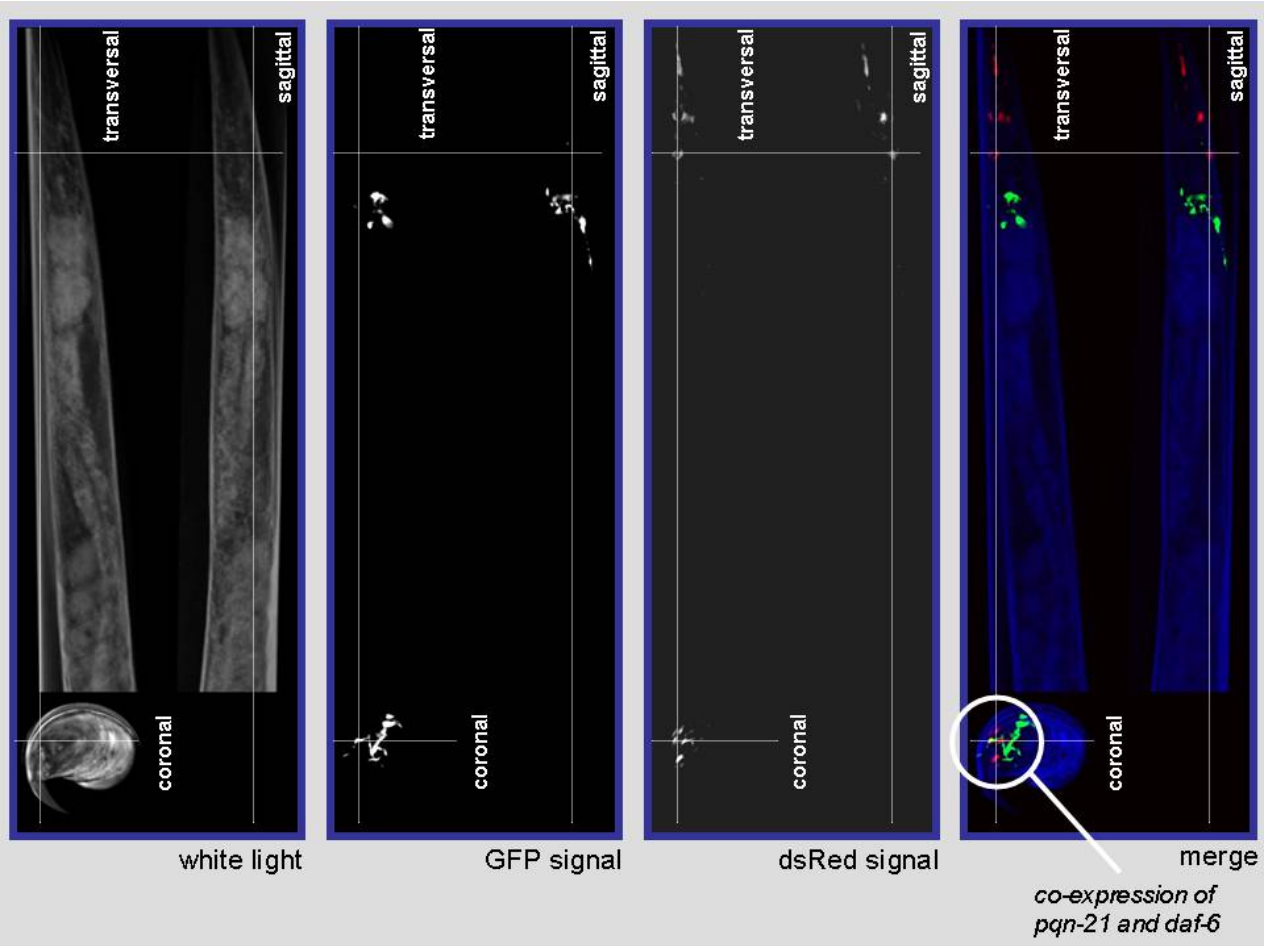

Figure 8: In silico *slice through* C. elegans*. White light image, GFP signal, dsRed signal and merge of 3D reconstructed data. GFP is expressed under the control of the* daf-6 *promoter and dsRed under the control of pqn-21 promoter. The merged picture shows a co-expression of the two fluorescent proteins in the pharynx-region. In this case slice 945 is shown in the coronal, transversal and sagittal view (see white line). Highlight of the neuron that shows co-expression.*

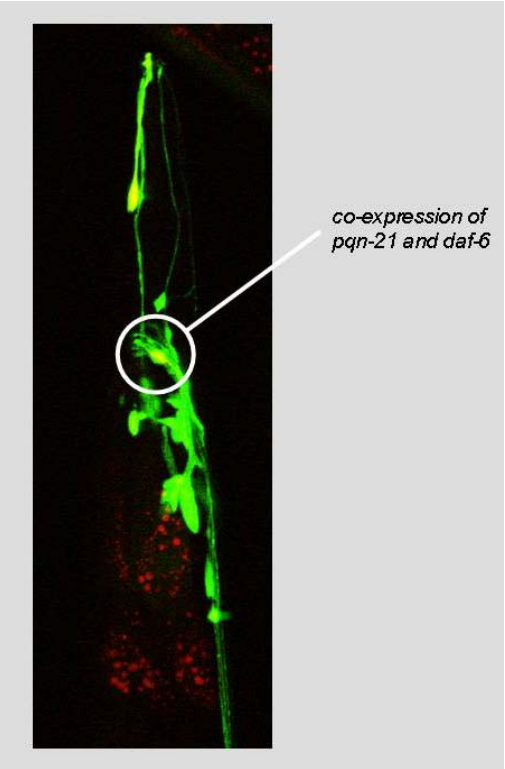

Figure 9: 2D Fluorescent microscopy of C. elegans*. GFP is expressed under the control of the* daf-6 *promoter and dsRed under the control of pqn-21 promoter. The merged picture shows a co-expression of the two fluorescent proteins in the pharynx-region of the nematode. Highlight of the neuron that shows co-expression.*

Discussion

The modified OPT set-up presented in this issue allows rapid *in vivo* 3D visualization in the widely used model organism *C. elegans*. The previously well-characterized anatomical features of the nematode are clearly visible in our recordings. Also, misdevelopment in mutant strains can be revealed in comparisson to wild type anatomical features. The white light images mainly serve as template for expression patterns of fluorescently labelled constructs. The expression patterns of GFP and GFP and dsRed co-expressed appear as expected in comparison to identifications previously done through confocal microscopy.

Nevertheless, the method still reveals some technical problems resulting in controversial results presented in this issue. The capillaries used in this study had to be pulled in order to make them as tiny as possible to perfectly accommodate and stabilize the nematode. The resulting conical form of the capillary makes the 3D reconstruction and especially digital clearance of the capillary wall more difficult. Further experiments will be done with already prepared capillaries with a smaller inner diameter which eventually will solve this problem.

Another issue is the stably fixation of the sample. Through anaesthetizing the worm with 10 mM NaN_3 unwanted movement is suppressed. Nevertheless, technical problems appeared with a constant movement of the capillary itself. These results in low quality 3D reconstruction data and in a blur final image and experiments have to be redone. Since movement of the capillary is constant through the whole record, the problematic can be overcome by modifying the reconstruction program with an algorithm. This addition to the program compensates the movement through all single recorded slices by taking the first and last image as templates and constantly correcting the recorded mistakes.

Due to those technical difficulties the recorded expression patterns are incomplete: the final resolution is not efficient enough to visualize GFP expression under the *unc-8* promoter in the axons of the according neurons and same counts for the *daf-6::GFP* and *pqn21::dsRed*. Co-localizations as observed through fluorescent light microscopy (see figure 9) can not be sufficiently visualized through OPT, although it was observed at least in one case (see figure 8). In principle, those malfunctions can be overcome in the future by solving the above mentioned problems and thereby making the technique more precise and reliable.

After all, OPT proves to be a true alternative to all other 3D imaging techniques visualizing *C. elegans* developed so far and therefore represents a powerful tool for general research in the nematode. Anatomical features and fluorescent gene expression patterns can be visualized and *in silico* sectioning of the animal is made possible in high resolution.

Another remarkable advantage is the possibility to record *C. elegans in vivo*. Animals die after a certain time due to the treatment with NaN_3 but due to their transparency they do not need to be fixed. Experiments with the anaestheticum levamisol have been performed. This drug does not lead to death of the animals but is not sufficient to suppress all the movement of the specimen which results in unusable reconstruction data. Nevertheless, varying the concentration of the drug might eventually lead to a complete immobilization of the animals. This would make records in certain time intervals possible, leading to developmental studies in *C. elegans*.

The method OPT has already been applied to several small size organisms and even to mouse, chick and human embryos. Several other animals can be recorded with this technique in the future, such as the embryos of the beetle *Tribolium castaneum* and the crustacean *Parhyale hawaiensis* and first according experiments have already been successfully performed (Averof personal communication).

Acknowledgements

My first and special thanks go to Heiko Meyer who created the used OPT setup and made a co-elaboration possible to perform recordings of *C. elegans*.
Further I thank my supervisor Prof. Dr. Nektarios Tavernarakis for his advice and support.
Special thanks to Dr. Jorge Ripoll for continuing the technical work with me in the recent months. He also acknowledges intensive discussion with J. Sharpe and M. Torres.
Thanks to Daphne Bazopoulou for providing the *C. elegans* strain expressing Ex[$_{daf\text{-}6}$GFP $_{pqn\text{-}21}$dsRed pRF4]. Further I would like to thank all the members of the Tavernarakis and Ripoll laboratories for their support.
This research was financed by E.U. Integrated Project “Molecular Imaging” LSHG-CT-2003-503259, E.U. STREP “TRANS-REG” LSHG-CT-2004-502950 and by grants from EMBO and the EU 6th.

References

Arques CG, Doohan R, Sharpe J, Torres M (2007) Cell tracing reveals a dorsoventral lineage restriction plane in the mouse limb bid mesenchyme. Development 134: 3713 - 3722

Bao Z, Murray JI, Boyle T, Ooi SL, Sandel MJ, Waterston RH (2006) Automated cell lineage tracing in Caenorhabditis elegans. Proc Natl Acad Sci U S A 103: 2707-2712

Bargmann CI, Avery L (1995) Laser killing of cells in Caenorhabditis elegans. Methods Cell Biol 48: 225-250

Bischoff M, Schnabel R (2006) Global cell sorting is mediated by local cell-cell interactions in the C. elegans embryo. Dev Biol 294: 432-444

Blumenthal T, Evans D, Link CD, Guffanti A, Lawson D, Thierry-Mieg J, Thierry-Mieg D, Chiu WL, Duke K, Kiraly M, Kim SK (2002) A global analysis of Caenorhabditis elegans operons. Nature 417: 851-854

Brenner S (1974) The genetics of Caenorhabditis elegans. Genetics 77: 71-94

Bryson-Richardson RJ, Berger S, Schilling TF, Cole NJ, Gibson AJ, Sharpe J, Currie PD (2007) FishNet: an online database of zebrafish anatomy. BMC Biology

Driscoll M, Gerstbrein B (2003) Dying for a cause: invertebrate genetics takes on human neurodegeneration. Nat Rev Genet 4: 181-194

Ellis HM, Horvitz HR (1986) Genetic control of programmed cell death in the nematode C. elegans. Cell 44: 817-829

Hall DH, Russell RL (1991) The posterior nervous system of the nematode Caenorhabditis elegans: serial reconstruction of identified neurons and complete pattern of synaptic interactions. J Neurosci 11: 1-22

Hird SN, White JG (1993) Cortical and cytoplasmic flow polarity in early embryonic cells of Caenorhabditis elegans. J Cell Biol 121: 1343-1355

Huisken J, Swoger J, Del Bene F, Wittbrodt J, Stelzer EH (2004) Optical sectioning deep inside live embryos by selective plane illumination microscopy. Science 305: 1007-1009

Hunt-Newbury R, Viveiros R, Johnsen R, Mah A, Anastas D, Fang L, Halfnight E, Lee D, Lin J, Lorch A, McKay S, Okada HM, Pan J, Schulz AK, Tu D, Wong K, Zhao Z, Alexeyenko A, Burglin T, Sonnhammer E, Schnabel R, Jones SJ, Marra MA, Baillie DL, Moerman DG (2007) High-throughput in vivo analysis of gene expression in Caenorhabditis elegans. PLoS Biol 5: e237

Jakubowski J, Kornfeld K (1999) A local, high-density, single-nucleotide polymorphism map used to clone Caenorhabditis elegans cdf-1. Genetics 153: 743-752

Jin Y (2005) C. elegans - A practical approach. Oxford University press

Kozlowski C, Srayko M, Nedelec F (2007) Cortical microtubule contacts position the spindle in C. elegans embryos. Cell 129: 499-510

Lee J, Nam S, Hwang SB, Hong M, Kwon JY, Joeng KS, Im SH, Shim J, Park MC (2004) Functional genomic approaches using the nematode Caenorhabditis elegans as a model system. J Biochem Mol Biol 37: 107-113

Lee K, Avondo J, Morrison H, Blot L, Stark M, Sharpe J, Bangham A, Coen E (2006) Visualizing Plant Development and Gene Expression in Three Dimensions Using Optical Projection Tomography. The Plant Cell 18: 2145-2156

Lim HY, Bodmer R, Perrin L (2006) Drosophila aging 2005/06. Exp Gerontol 41: 1213-1216

McGurk L, Morrison H, Keegan LP, Sharpe J, O'Connell MA (2007) Three-Dimensional Imaging of *Drosophila melanogaster*. PLoS ONE

Mello C, Fire A (1995) DNA transformation. Methods Cell Biol 48: 451-482

Mello CC, Conte D, Jr. (2004) Revealing the world of RNA interference. Nature 431: 338-342

Murakami S (2007) Caenorhabditis elegans as a model system to study aging of learning and memory. Mol Neurobiol 35: 85-94

Paddock SW (1999) Confocal laser scanning microscopy. Biotechniques 27: 992-996, 998-1002, 1004

Pautler RG, Fraser SE (2003) The year(s) of the contrast agent - micro-MRI in the new millennium. Curr Opin Immunol 15: 385-392

Perens EA, Shaham S (2005) C. elegans daf-6 encodes a patched-related protein required for lumen formation. Dev Cell 8: 893-906

Riddle DL, Blumenthal T, Meyer BJ, Priess JR (1997) C. elegans II. Cold Spring Harbor Laboratory Press, New York II

Ripoll J, Ntziachristos V (2004) Imaging Scattering media from a distance: theory and applications of non-contact optical tomography. Modern Physics Letters B 18

Sarma S, Kerwin J, Puelles L, Scott M, Strachan T, Feng G, Sharpe J, Davidson D, Baldock R, Lindsay S (2005) 3D modelling, gene expression mapping and post-mapping image analysis in the developing human brain. Brain Res Bull 66: 449-453

Sarov M (personal communication) In:

Schmitz C, Kinge P, Hutter H (2007) Axon guidance genes identified in a large-scale RNAi screen using the RNAi-hypersensitive Caenorhabditis elegans strain nre-1(hd20) lin-15b(hd126). Proc Natl Acad Sci U S A 104: 834-839

Schnabel R (2005) C. elegans - A practical approach. Oxford University press

Schnabel R, Bischoff M, Hintze A, Schulz AK, Hejnol A, Meinhardt H, Hutter H (2006) Global cell sorting in the C. elegans embryo defines a new mechanism for pattern formation. Dev Biol 294: 418-431

Schnabel R, Hutter H, Moerman D, Schnabel H (1997) Assessing normal embryogenesis in Caenorhabditis elegans using a 4D microscope: variability of development and regional specification. Dev Biol 184: 234-265

Sharpe J (2003) Optical projection tomography as a new tool for studying embryo anatomy. Journal of Anatomy 202: 175 - 181

Sharpe J, Ahlgren U, Perry P, Hill B, Ross A, J. H-S, Baldock R, Davidson D (2002) Optical projection tomography as a tool for 3D microscopy and gene expression studies. Science 296: 541-545

Simmer F, Moorman C, van der Linden AM, Kuijk E, van den Berghe PV, Kamath RS, Fraser AG, Ahringer J, Plasterk RH (2003) Genome-wide RNAi of C. elegans using the hypersensitive rrf-3 strain reveals novel gene functions. PLoS Biol 1: E12

Sulston JE, Schierenberg E, White JG, Thomson JN (1983) The embryonic cell lineage of the nematode *Caenorhabditis elegans*. Dev. Biol. 100: 64-119

Tavernarakis N, Shreffler W, Wang S, Driscoll M (1997) unc-8, a DEG/ENaC family member, encodes a subunit of a candidate mechanically gated channel that modulates C. elegans locomotion. Neuron 18: 107-119

Tavernarakis N, Wang SL, Dorovkov M, Ryazanov A, Driscoll M (2000) Heritable and inducible genetic interference by double-stranded RNA encoded by transgenes. Nat Genet 24: 180-183

Thomas JH, Lockery S (2005) In C. elegans - A practical approach: Neurobiology. Oxford University press

Walhout AJ, Sordella R, Lu X, Hartley JL, Temple GF, Brasch MA, Thierry-Mieg N, Vidal M (2000) Protein interaction mapping in C. elegans using proteins involved in vulval development. Science 287: 116-122

Waterston R, Sulston J (1995) The genome of Caenorhabditis elegans. Proc Natl Acad Sci U S A 92: 10836-10840

White JG, Southgate E, Thomson JN, Brenner S (1983) Factors that determine connectivity in the nervous system of Caenorhabditis elegans. Cold Spring Harb Symp Quant Biol 48 Pt 2: 633-640